Journal of Applied Polymer Science

Processing and characterization of bio-based poly (hydroxyalkanoate)/poly(amide) blends: Improved flexibility and impact resistance of PHA-based plastics

Shengzhe Yang,[1] Samy A. Madbouly,[1,5] James A. Schrader,[2] David Grewell,[3] Michael R. Kessler,[4] William R. Graves[2]

[1]Department of Materials Science and Engineering, Iowa State University, Ames, Iowa
[2]Department of Horticulture, Iowa State University, Ames, Iowa
[3]Department of Agriculture and Biosystems Engineering, Iowa State University, Ames, Iowa
[4]School of Mechanical and Materials Engineering, Washington State University, Pullman, Washington
[5]Department of Chemistry, Faculty of Science, Cairo University, Orman-Giza, Egypt
Correspondence to: S. A. Madbouly (E-mail: madbouly@iastate.edu)

ABSTRACT: One of the most significant limitations to widespread industrial implementation of emerging bioplastics such as poly(lactic acid) and poly(hydroxyalkanoate) (PHA) is that they do not match the flexibility and impact resistance of petroleum-based plastics like poly(propylene) or high-density poly(ethylene). The basic goal of this research is to identify alternative, affordable, sustainable, biodegradable materials that can replace petroleum-based polymers in a wide range of industrial applications, with an emphasis on providing a solution for increasing the flexibility of PHA to a level that makes it a superior material for bioplastic nursery-crop containers. A series of bio-based PHA/poly(amide) (PA) blends with different concentrations were mechanically melt processed using a twin-screw extruder and evaluated for physical characteristics. The effects of blending on viscoelastic properties were investigated using small-amplitude oscillatory shear flow experiments to model the physical character as a function of blend composition and angular frequency. The mechanical, thermal, and morphological properties of the blends were investigated using dynamic mechanical analysis, differential scanning calorimetry, thermogravimetric analysis, scanning electron microscopy, and tensile tests. The complex viscosity of the blends increased significantly with increasing concentration of PHA and reached a maximum value for 80 wt % PHA blend. In addition, the tensile strength of the blends increased markedly as the content of PHA increased. For blends containing PA at >50 wt %, samples failed only after a very large elongation (up to 465%) without significant decrease in tensile strength. The particle size significantly increased and the blends became more brittle with increasing concentration of PHA. In addition, the concentration of the PA had a substantial effect on the glass relaxation temperature of the resulting blends. Our results demonstrate that the thermomechanical and rheological properties of PHA/PA blends can be tailored for specific applications, and that blends of PHA/PA can fulfill the mechanical properties required for flexible, impact-resistant bio-based nursery-crop containers.
 J. Appl. Polym. Sci. **2015**, *132*, 42209.

KEYWORDS: biodegradable; bioengineering; biopolymers & renewable polymers; blends

Received 23 November 2014; accepted 9 March 2015
DOI: 10.1002/app.42209

INTRODUCTION

The use of petroleum-based plastics for products and packaging has become ubiquitous in industry, a trend that is contributing heavily to ecological problems such as increased CO_2 levels, pollution of land and waterways, and overloading of the solid-waste stream. Although petroleum plastics are extremely versatile and fulfill the performance requirements for a multitude of applications, increasing public awareness of their environmental impacts has spurred efforts to replace petroleum feedstocks with sustainable and ecofriendly alternatives.[1–15] Motivated by the goal to reduce our carbon footprint and dependence on fossil carbon sources, bio-based polymers and composites are becoming widely utilized in polymer manufacturing and medical applications.[16–18] One area of strong interest is the replacement of petroleum-based plastics with bioplastics in horticulture containers used by the nursery-crops industry. Although interest is high, the industry has struggled to develop a bio-based container that can fulfill the functional requirements for

long-term nursery-crops production. Many of the difficulties are related to poor flexibility and low impact resistance of materials that cannot withstand the harsh treatment encountered during use.

The poly(hydroxyalkanoates) (PHAs) most widely used in industry are aliphatic thermoplastic poly(esters) synthesized via metabolic pathways of microorganisms by fermentation of sugars or lipids.[19] PHAs containing over 90 types of monomers have been synthesized in various microorganisms. The characteristics of thermoplastic PHAs range from rigid plastics to tough elastomers and depend on their molecular structure. Specifically, the properties of PHAs are highly dependent on the copolymer composition. Generally, thermoplastic PHAs are rigid but brittle, with poor impact resistance and flexibility, issues that restrict the applications for which PHAs can be used as alternatives to traditional petroleum-based plastics. Copolymers of 4-hydroxybutyrate and 3-hydroxybutyrate can be synthesized to produce bio-based polymers with different mechanical and thermal properties. Poly(3-hydroxybutyrate) is a brittle semi-crystalline material with crystallinity $\geq$50% and T_g of approximately 4°C. However, poly(4-hydroxybutyrate) is more elastic with very low crystallinity and $T_g = -48$°C. Most of the efforts aimed at improving the toughness of PHA have focused on blending PHA with other polymers such as poly(lactide) or thermoplastic starch.[19–22] The majority of reports regarding PHA blends focus on only a few aspects of their character, such as viscoelastic or rheological properties, instead of providing a comprehensive characterization of the material, and there have been no investigations evaluating the blending of poly(amide) with PHA to improve its flexibility and impact resistance for increased industrial application.

Poly(amide) (PA) is a resin containing monomers of amides joined by peptide bonds, and can be made artificially through step-growth polymerization or solid-phase synthesis. PA has been used in blends with various polymers such as poly(lactide) to facilitate a good combination of toughness and stiffness.[23] Hydrogen bonding between the molecules results in good mechanical performances in both crystalline and amorphous states. The PA used in this study is a bio-derived resin that is manufactured from tall oil and processed through dimerization and polycondensation. Tall oil is a viscous yellow-black liquid that can be obtained from pine tree and is a by-product of the pulp and paper industry. This bio-based PA has high viscosity, low softening temperature, high flexibility, and high water resistance and is widely used in industrial applications such as, adhesives, ink binders, and coatings. All polymers used in this study were commercially available and bio-based.

The objectives of our research were (1) to quantify the effects of blending PA with PHA; (2) to characterize the thermal, morphological, rheological, and mechanical properties of PHA/PA blended at three different load ratios (80/20, 50/50, and 20/80); and (3) to compare the material properties of these PHA/PA blends with those of neat PHA and neat PA. Results were examined to assess the suitability of using PHA/PA blends in the model application of bio-based nursery-crop containers that could provide equal function to that of petroleum-plastic containers.

EXPERIMENTAL

Materials

Poly(hydroxyalkanoate) Mirel P1003 (compression molding grade resins) was supplied by Metabolix Inc., Cambridge, MA 02139. This PHA is made by fermentation of renewable bio-based feedstock, making it fully bio-based in neat form. Mirel P1003 is a blend of PHB and poly(3-hydroxybutyrate-*co*-4-hydroxybutyrate). The poly(amide) UNI-REZ^{TM} 2651 was obtained from Arizona Chemical Inc., Jacksonville, FL, and is a fully bio-based resin derived from tall oil of pine tree.

Microcompounding and Compression Molding

Complete drying of PHA and PA was accomplished by heating the material in a vacuum oven for 8 h at 60°C. The desired amounts of PHA and PA granules were fed into a twin-screw microcompounder (DACA Instrument, Santa Barbara, CA) set to 185°C and a rotation speed of 100 rpm. The mixing time was controlled for 10 min to facilitate homogenous melt compounding. The extruded materials were then compression molded at 185°C to prepare the samples for dynamic mechanical analysis (DMA).

Measurements

Scanning Electron Microscopy. The fracture surface morphology of PHA/PA blends (wt % ratios of 20/80, 50/50, and 80/20) was examined using scanning electron microscopy (SEM). The tensile-fractured samples were fixed on the SEM holders after sputter coating with a thin gold layer. The prepared samples were characterized using a field-emission scanning electron microscope (FE-SEM, FEI Quanta 250) operating at 10 kV under high vacuum.

Rheological Measurements. The rheological properties of blends were investigated under an AR2000ex rheometer (TA Instruments, New Castle, DE) with parallel plates of 25 mm diameter. All measurements were performed under temperature accuracy of ±0.1°C. A platinum resistance thermometer (PRT) sensor positioned at the center of the plate ensured optimum temperature stability and control. The rheological experiments were studied on angular frequency sweeps at 180°C to evaluate the complex viscosity and shear storage modulus. All measurements of PHA/PA blends (wt % ratios of 20/80, 50/50, and 80/20) were examined and compared in frequency sweep testing mode.

DMA Measurements. The DMA was performed with a DMA Q800 dynamic mechanical analyzer from TA Instruments. All samples were measured with a film-tension mode of 1 Hz. Rectangular specimens of 0.9 × 5 mm (thickness × width) were used for the analysis. All the samples were heated to 200°C and annealed for 3 min to remove the thermal history before any measurements. The samples were cooled and held isothermally for 3 min at −100°C before the temperature was increased to 100°C at a rate of 3°C/min.

DSC Measurements. Differential scanning calorimetry (DSC) measurements were performed using a thermal analyzer (TA Instrument Q2000) to study the melting and crystallization behavior of PHA/PA blends. All DSC measurements were carried out in nitrogen atmosphere. The samples were heated from

room temperature to 200°C at a heating rate of 20°C/min to erase their anterior thermal history, equilibrated at 200°C for 3 min, and then cooled to room temperature at a cooling rate of 20°C/min. The crystallization temperature (T_c) was evaluated using the exothermic crystallization peak. The samples were then reheated to 200°C at the same constant rate, measuring the second heating curves as well as the cooling curves. The melting temperature (T_m) of all samples was determined from the maximum of the endothermic melting peak. Samples of 5 mg were cut from the films and used for analysis.

TGA Measurements. A Q50 thermogravimetric analyzer (TGA) from TA Instruments was employed to investigate the thermal stability of PHA/PA blends. The samples were heated from room temperature to 600°C at a heating rate of 20°C/min under nitrogen atmosphere. Generally, 20 mg samples were used for the TGA.

Mechanical Properties

The tensile performance of the samples was determined using an Instron universal testing machine at an extension rate of 50.0 mm/min using a static load cell (±2 kN). Rectangular specimens of 50 × 10 mm (length × width) were used. All samples had the same processing and thermal history. Average values were calculated from at least three replicates of each sample. The toughness of the polymer was determined from the area under the corresponding tensile stress–strain curves.

RESULTS AND DISCUSSION

SEM is a well-established technique that is widely employed to investigate the internal structure or morphology of biodegradable polymers.[24–27] For the PHA/PA blends, the fracture surface morphology was investigated for the different weight ratios (20/80, 50/50, and 80/20). The facture morphologies of specimens after tensile testing are shown in Figure 1(a). Two-phase structure is clearly observed for different blend compositions. A relatively smooth surface topography was observed for the PHA/PA (20/80) blend. With increasing PHA content, the particle size significantly increased and the surface eroded and was etched with well-defined pits. For samples with PHA at 50 wt %, the spherical particles of PHA were pulled out from the surface, which showed strong interfacial adhesions of the two phases. With the PHA content at 80 wt %, the blend agglomerated into large (ca 60–80 μm) individual irregular pieces during melt compounding. In addition, the blends became more brittle with increasing concentration of PHA.

SEM micrographics for the PHA/PA (80/20) blend are shown at different magnifications in Figure 1(b). The landform on the fracture surface was disorderly and resembled unsystematic crushed aggregates. The two components appeared completely separated and broken into small particles, because the final mechanical properties of composites are highly dependent on their morphology.[23,28,29] The fragile character of the PHA/PA (80/20) blend is due to the macrophase separation of the blend and the poor interfacial adhesion between the two polymer components. This consequently led to difficulty in testing the tensile strength of this specific specimen.

We hypothesized that the weight percent ratio of the PHA/PA blends would have a significant influence on the viscoelastic properties. For this reason, the rheological behavior of this blend was studied as a function of classical angular frequency by using small-amplitude oscillatory shear flow experiments. Figure 2(a) compares the effect of dynamic angular frequency on the viscoelastic behavior in PHA/PA blends, showing the dependence of complex viscosity, η^*, at the same temperature, 180°C. The viscosity of pure PHA is almost angular frequency independent (Newtonian behavior), while the viscosity of pure PA and all blends showed non-Newtown behavior (i.e., the viscosity decreased with increasing angular frequency). In addition, η^* increased significantly for blends with 20 and 50 wt % PA and then decreased for 80 wt % PA. This behavior is mainly attributed to the different morphologies developed in the melt processing of the blends as clearly seen in Figure 1. The microstructured two-phase morphology observed for blends with 20 and 50 wt % PA acts as a reinforcement polymer composite and consequently the dynamic viscosity increased significantly.[30] The particle size of the phase-separated structure decreases dramatically for the blend with 80 wt % PA and the viscosity decreased due to the high compatibility between the two polymer components. Figure 2(b) shows the composition dependence of complex viscosity at 180°C and different angular frequencies. Clearly the viscosity decreases with increasing angular frequency and attains a maximum for 20 wt % PA blend as aforementioned.

The effect of blend ratio of PHA and PA on the dynamic mechanical properties of the material was investigated in the temperature range from −100 to 100°C. The variation of the storage modulus (E') and loss tangent (tan δ) of the pure PHA, PA, and their blends are shown in Figure 3. The sample of PHA/PA (80/20) was not included because it was too brittle to prepare reliable dimensions for the DMA measurements. As illustrated in Figure 3(a), the storage modulus at the glassy region decreased markedly as the amount of PA increased. With increasing PA loadings up to 50 wt %, the storage modulus of the PHA/PA blends showed a noticeable decrease to nearly one-third that of the neat PHA. At the rubbery plateau, this trend became more prominent. When the temperature elevated above 50°C, the storage modulus of the blends decreased much more than that of the pure PHA. At higher temperatures ($T \geq 75$°C), E' decreased very sharply due to the slippage of large-scale molecular chains.[20,31]

In general, the glass transition temperature (T_g) can be measured using several experimental techniques, such as DSC, DMA, TMA, and broadband dielectric spectroscopy. Determination of T_g of blends with large mismatch in their T_gs can be used to evaluate the degree of miscibility of the two polymer components. Normally a single T_g can be detected for miscible blends while two T_gs for immiscible or partially miscible blends. It is also known that relaxation peak from DMA can be directly associated with the T_g of the material as well as to the drop of storage tensile modulus.[32] The tan δ curve of the PHA/PA blends as a function of blend composition is presented in Figure 3(b). The concentration of the PA had a considerable effect on the glass relaxation temperature of the resulting blends. The tan

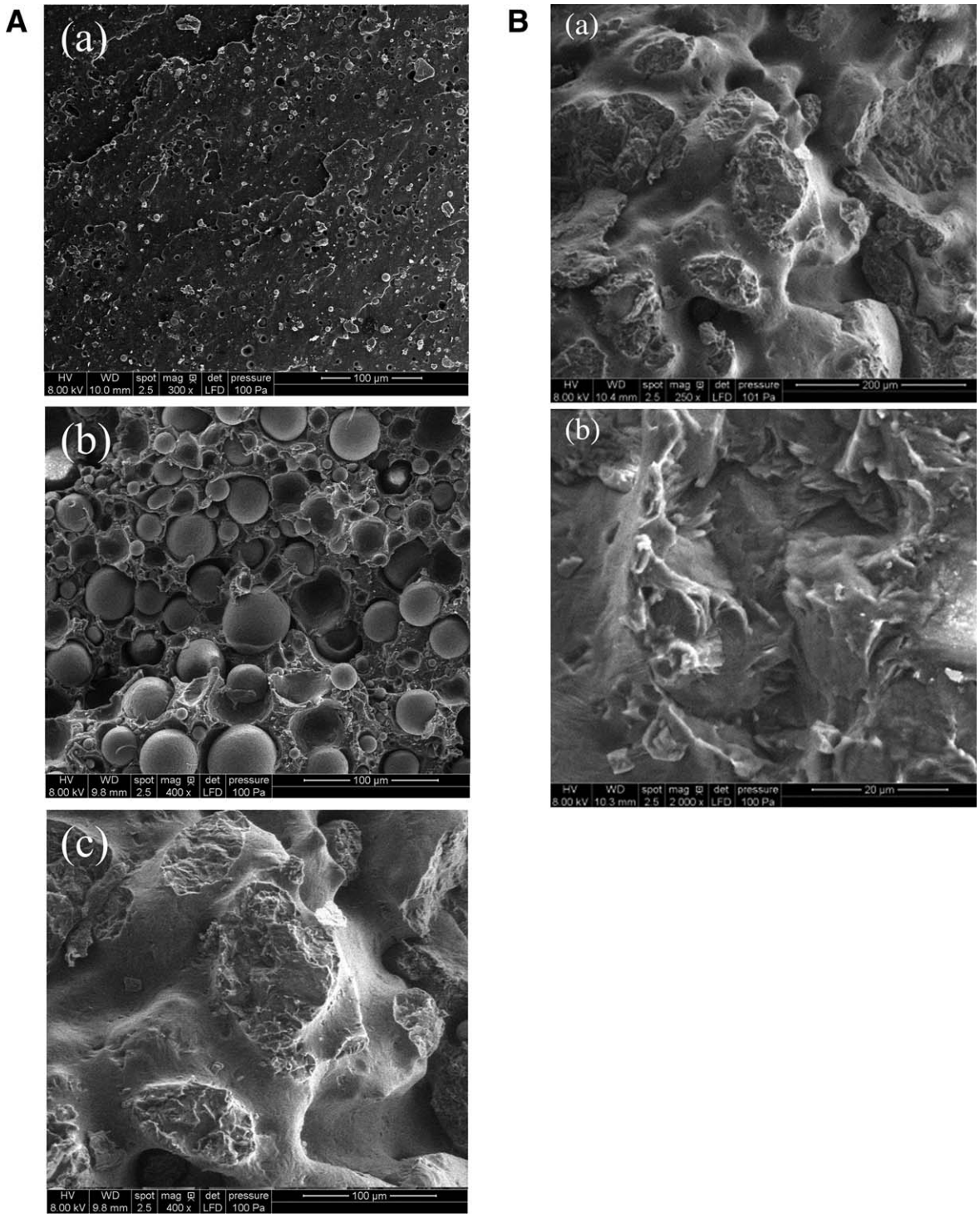

Figure 1. (A) SEM images for fracture surface morphologies of PHA/PA blends (a) PHA/PA (20/80); (b) PHA/PA (50/50); (c) PHA/PA (80/20). (B) SEM micrographs for fracture surface morphology of PHA/PA (80/20) at (a) 250× and (b) 2000× magnification.

δ peak magnitudes of blends decreased after the loading of PA, a result related to the modulus drop. Meanwhile, the position of the relaxation peak shifted toward lower temperatures with increasing PA content. Consequently, based on the position of relaxation peak, T_g of the blended material became lower as the amount of PA increased due to the partial miscibility of the two polymer components.

DSC was used to measure the temperatures and heat flow during thermal transitions of PHA/PA blends. The crystallization behavior of semicrystalline polymers has a substantial effect on their mechanical properties, and the second-phase additives affect the crystallinity of the binary polymer blends.[23,33,34] The DSC traces for PHA/PA blends during the second heating scan as a function of blend composition are shown in Figure 4. The

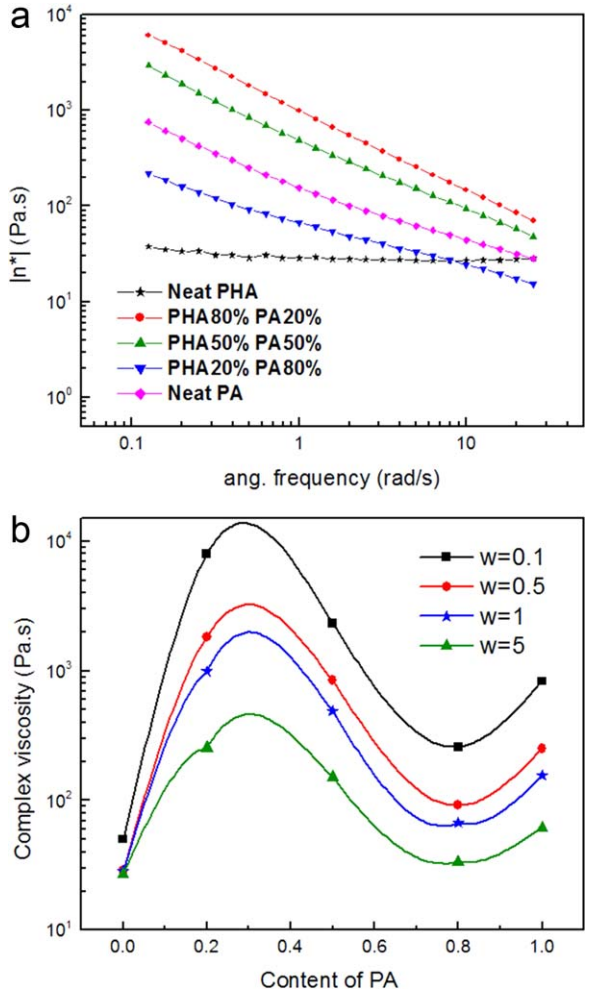

Figure 2. (a) Angular frequency dependence of η^* for PHA/PA blends at 180°C. (b) Composition dependence of η^* for PHA/PA blends at 180°C for different angular frequency. [Color figure can be viewed in the online issue, which is available at wileyonlinelibrary.com.]

first heating process, from room temperature to 200°C at a heating rate of 20°C/min, was used to erase thermal and mechanical histories. For the pure PHA, PHA/PA (80/20), and PHA/PA (50/50), the curves displayed two endothermic peaks due to primary and secondary crystallization processes. These double melting peaks were found after the complete crystallization cooling from the melting indicated and confirmed the existence of melt-recrystallization mechanisms.[35–38] The less perfect crystals melted at lower temperature, and then at a higher temperature, the sample reorganized into more perfect crystals and remelted during the heating process. Table I compares the melting enthalpy (ΔH_m) and melting temperature (T_m) of PHA, PHA/PA (80/20), and PHA/PA (50/50), showing that the melting points of the blends decreased as the concentration of poly(amide) increased. The ΔH_m was calculated by integrating the area of two bimodal melting peaks. As a function of blend composition, ΔH_m decreased significantly with increasing poly(amide) content as seen from the data in Table I. No endothermic melt peaks were observed in the DSC curves for pure PA or PHA/PA (20/80), indicating that no apparent crystallization process took place within the temperature range of room temperature to 200°C. Consistent with the results observed for ΔH_m and T_m, the DSC curves showed a similar declining trend, indicating that the amorphous properties of PA reduced the crystallization of PHA/PA blends and diminished the appearance of the melting peak.

The DSC analysis was also carried out to determine the release of heat in the exothermic cold crystallization process of PHA/PA blends. Latent heat is released during the phase change, and this macroscopic process is closely related to the rate of the crystallization process.[39,40] The DSC thermograms for PHA/PA blends during the first cooling scan as a function of blend composition are shown in Figure 5. Noticeable are the results for blends containing higher PHA loadings that exhibit sharper and more intense peaks than the others. The pure PHA underwent a well-defined cold crystallization process with the peak of cold crystallization temperature (T_c) at approximately 108°C. Likewise, PHA/PA (80/20) and PHA/PA (50/50) blends show similar character of crystallization activity. The values for cold

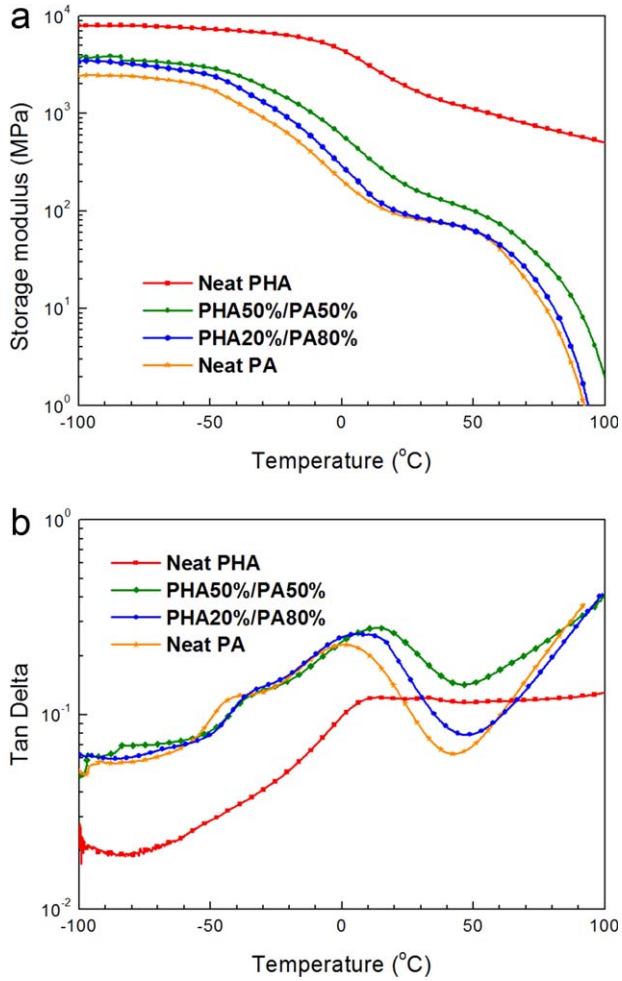

Figure 3. (a) Temperature dependence of dynamic storage moduli, E' of the PHA/PA blends as a function of blend composition. (b) Temperature dependence of tan δ curves of the PHA/PA blends as a function of blend composition. [Color figure can be viewed in the online issue, which is available at wileyonlinelibrary.com.]

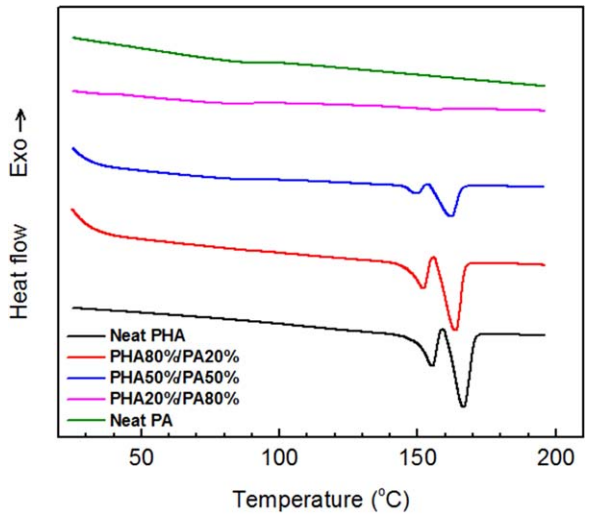

Figure 4. DSC heating scan for PHA/PA blends. The DSC measurements were carried out at 20°C/min heating rate (second heating run). [Color figure can be viewed in the online issue, which is available at wileyonlinelibrary.com.]

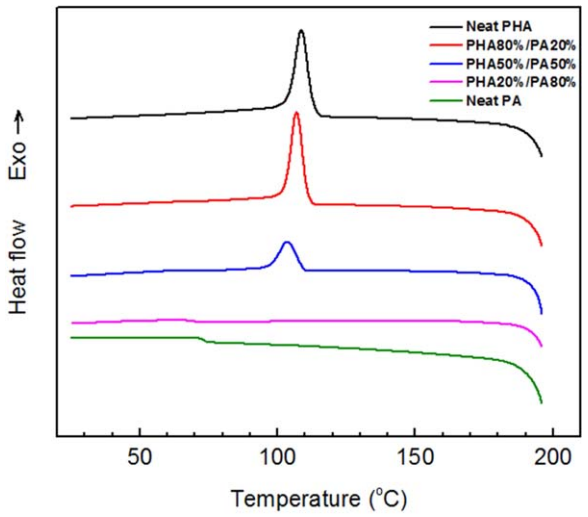

Figure 5. DSC cooling scan for PHA/PA blends. The DSC measurements were carried out at a cooling rate of 20°C/min (first cooling run). [Color figure can be viewed in the online issue, which is available at wileyonlinelibrary.com.]

crystallization enthalpy (ΔH_c) and cold crystallization temperature (T_c) for PHA, PHA/PA (80/20), and PHA/PA (50/50) decreased systematically as the concentration of the poly(amide) increased (Table I).

It is well established that the mechanical and physical properties of amorphous/semicrystalline polymer blends are greatly influenced by crystallization kinetics and degree of crystallinity as well as microstructure or morphology of the blends. The nature of interaction, miscibility, and internal structure of the blends normally have a major impact on the degree of crystallinity and ultimate mechanical properties of the amorphous/semicrystalline blends. Generally, higher crystallinity results in an increase in the stiffness (elastic modulus) and strength of the polymer, while ductility declines significantly. For the current system, the bio-derived tall oil-based PA is totally amorphous; however, most of petroleum-based PAs are semicrystalline. The bacterial-based PHA is a semicrystalline polymer with a degree of crystallinity of approximately 23% as measured by DSC. Blending PA with PHA likely has a significant influence on the degree of crystallinity of PHA and consequently on the ultimate mechanical properties of the blends. For this reason, the degree of crystallinity (X_c) of PHA/PA bends was estimated from the melting enthalpies determined by calorimetry. The higher the crystallinity, the more melting heat required to destroy the crystal structure. X_c was ascertained by eq. (1),[41] considering a melting enthalpy of 142 J/g for 100% crystalline PHB as cited in the literature.[42,43]

$$X_c = \frac{\Delta H_m}{W_p \times \Delta H_{m100\%}} \times 100\% \quad (1)$$

where X_c is the crystallinity (%), ΔH_m is the melting enthalpy of the polymer (J/g), W_p is the proportion of the polymer in the blend, and $\Delta H_{m100\%}$ is the melting enthalpy of the 100% crystalline polymer.

Table I. Summary of Melting Enthalpy, Melting Temperature, Cold Crystallization Enthalpy, Cold Crystallization Temperature, Degree of Crystallinity, and T_g from tan δ of PHA and PHA/PA Blends Under Nitrogen Atmosphere

	Neat PHA	PHA/PA (80/20)	PHA/PA (50/50)
ΔH_m (J/g)	32.30	25.45	10.78
T_m (°C)	166.48	162.76	161.59
ΔH_c (J/g)	30.52	23.61	10.72
T_c (°C)	108.76	107.13	103.65
X_c (%)	22.75	22.40	15.18
T_g (°C)	17		14

The PHA/PA 20/80 blend and pure PA are amorphous and have T_gs of 7 and −2°C, respectively.

On the basis of results in Table I, the degree of crystallinity depends substantially on the blend composition. Specifically, the degree of crystallinity decreased with increasing PA concentration. Overall, the quantity of amorphous substance resulted in an overall decrease in the crystallization behavior.

In general, the mechanical properties of binary polymer blend systems are useful and very important for industrial applications.[44] Tensile strength is an important mechanical parameter for materials that are designed to be stretched or under tension. Material toughness can be considered as tensile toughness and impact strength.[45] Fracture behavior of PHA, PA, and PHA/PA blends in the tensile test varied significantly from brittle fracture of pure PHA to ductile fracture of pure PA, results that are illustrated in the stress–strain curves in Figure 6. The sample of PHA/PA (80/20) was not included because it was too brittle to prepare reliable dimensions for the tensile test. The fragile character of this blend is mainly attributed to the very poor miscibility and weak interfacial adhesion between the two polymers [Figure 1(c)] when PHA is a major component. Neat PHA showed a distinct yield point with a subsequent strain

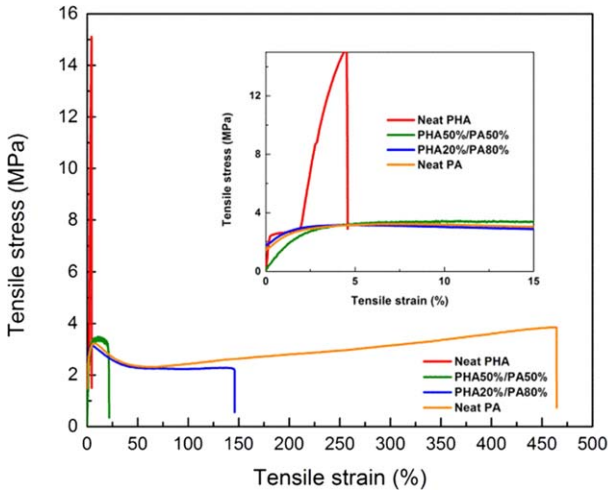

Figure 6. Comparison of tensile stress–strain curves of PHA/PA blends. The inset-plot gives details of the mechanical testing data from 0 to 15% tensile strain. [Color figure can be viewed in the online issue, which is available at wileyonlinelibrary.com.]

hardening stage before failure, character resulting from its two components as described in the materials section. Its strain at break was only around 4.6%, as illustrated in Figure 6. When the concentration of PA in the blend was more than 50 wt %, the PHA/PA blends showed noticeable ductile characteristics with the appearance of distinct yielding and neck formation.

The effects of PA content on the mechanical properties of PHA/PA blends are depicted in Figure 7, which shows that the tensile strength of specimens decreased systematically as the content of PA increased. When the content of PA was <50 wt %, the elongation of the blend increased slightly, while tensile strength declined significantly. Above 50 wt % of PA, the samples failed at very large elongation, which increased greatly from 22% for the 50/50 blend to 465% for pure PA without obvious decrease

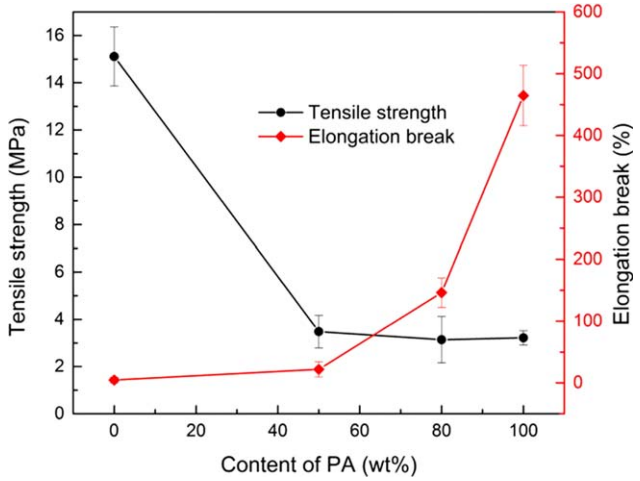

Figure 7. Composition dependence of tensile strength and elongation at break % for PHA/PA blends with different PA concentrations. The error bars represent standard deviations based on three repeated measurements. [Color figure can be viewed in the online issue, which is available at wileyonlinelibrary.com.]

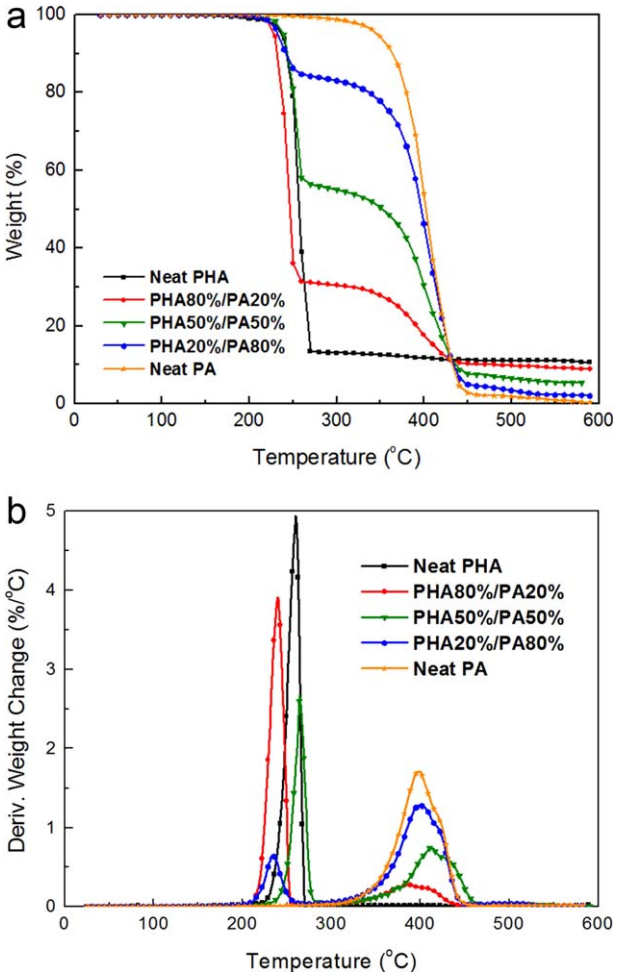

Figure 8. (a) Temperature dependence of weight loss % for different PHA/PA blends at 20°C/min under nitrogen atmosphere. (b) Comparison of first derivative weight changes of the PHA/PA blends at 20°C/min under nitrogen atmosphere. [Color figure can be viewed in the online issue, which is available at wileyonlinelibrary.com.]

of the tensile strength. The mechanical properties of PHA/PA blends can be explained based on the degree of crystallinity. The substantial decrease in the tensile strength and increase in the elongation at break with increasing PA content are attributed to the fact that the degree of crystallinity decreased with increasing PA content in the blend. As presented in Table I, the degree of crystallinity decreased from about 23% for pure PHA to 15% for the PHA/PA (50/50) blend. In addition, no melting or crystallization peaks were observed for pure PA and the PHA/PA (20/80) blend, indicating that they are totally amorphous (Figures 4 and 5).

It is also well known that combination of desirable mechanical and physical properties of certain polymer blends can be obtained by controlling the processing condition and morphology. The mechanical properties (e.g., tensile strength, tensile modulus, and impact toughness) of polymer blends with droplet morphology are typically much lower than that with fiber-like structure morphology. For our system, droplet morphology of PHA dispersed phase in PA matrix has been observed for

Table II. Summary of Thermogravimetric Analysis of PHA/PA Blends Under Nitrogen Atmosphere

	Neat PHA	PHA/PA (80/20)	PHA/PA (50/50)	PHA/PA (20/80)	Neat PA
T_{10} (°C)	252.75	233.30	245.07	241.78	364.09
T_{50} (°C)	265.28	246.38	352.46	396.96	402.29
T_{max} (°C)	267.09	244.69	253.85	404.13	403.34

PHA/PA (20/80) and (50/50) blends [Figure 1(a)]. The PHA/PA (50/50) blend has larger particle size than that of PHA/PA (20/80) blend. These two blends have slight difference in the mechanical properties as seen in Figure 7. Since both of these blends have droplet structure, the effect of morphology on the mechanical properties is very minor compared to the effect of crystallinity. The lower tensile strength and higher elongation at break for PHA/PA (20/80) blend compared to PHA/PA (50/50) blend are mainly attributed to the fact that, PHA/PA (20/80) is amorphous, while PHA/PA (50/50) is crystalline. The PHA/PA (80/20) blend has very poor mechanical properties due to the macrophase separation of the two components. In addition, the blend is very brittle, and no reliable sample specimen could be prepared to measure the tensile properties. Based on the above, it is apparent that the morphology of the PHA/PA blends has insignificant influenced on the mechanical properties.

The thermal degradation behavior of PHA/PA blends was studied by TGA, which uses heat to induce chemical and physical changes in materials and performs a corresponding measurement of mass change as a function of temperature. The TGA profile, as seen from Figure 8, suggests that decomposition started during melting and terminated with a weight loss corresponding to the content of blend composition. It was found that the pure PHA and pure PA degraded in a one-stage process, while the PHA/PA blends showed a very distinct two-stage degradation pattern. The blends experienced significant weight loss between 250 and 450°C (Figure 8a), with the weight-loss peaks at approximately 250 and 400°C (Figure 8b). Above 600°C, no obvious further weight loss was observed during pyrolysis in inert nitrogen atmosphere.

Table II compares the degradation temperatures of PHA/PA blends at different percentage weight loss. T_{10} denotes the temperature at which the samples lost 10% of their original mass. On the basis of these data, PA exhibited higher thermal resistance arising from amide linkages, which result in stiff macromolecular chains that interact with each other via strong hydrogen bonds.[46,47] The degradation temperature at 50% weight loss (T_{50}) was also investigated for PHA, PA, and PHA/PA blends, and the T_{50} value for each blend was roughly the same as its T_{max}, the maximum degradation temperature. It is evident from the thermogram [Figure 8(a)] that T_{max} was enhanced with increasing concentration of PA, which indicates that the thermal stability of PHA-based materials can be improved by blending with PA.

Blends of PHA/PA have strong potential for use in biocontainers for the nursery-crop industry. Unlike the greenhouse industry, which normally produces plants with crop cycles <12 weeks and often uses containers held in shuttle trays, the nursery industry produces species with medium- and long-term crop cycles commonly more than a year long, and containers are often handled individually, requiring them to exhibit greater flexibility and impact resistance and a moderate biodegradation rate. Along with improved mechanical properties obtained by blending PA with PHA, PA can function to reduce the rate of biodegradation compared to pure PHA.[48] Although the mechanical properties of neat PA are suitable for use of the material in horticulture containers without a copolymer, neat PA is currently much more expensive than PHA (approximately $8.60 and $4.40 USD per kg, respectively), making it cost-prohibitive to use neat PA for this application. Blending PA with lower cost polymers like PHA provides a material with some of the advantages of PA, at a more reasonable cost than neat PA resin. Compared to the cost of the petroleum-based plastic commonly used for this application (high-density poly(-ethylene) (HDPE)), the current costs of PHA/PA blends are approximately double the price. While the cost of PHA/PA material is greater than that of HDPE at the present time, there are two factors that indicate that horticulture containers made of PHA/PA may be cost competitive with HDPE in the near future. (1) Economists specializing in horticultural strategies have determined that many consumers would be willing to pay $0.23 to $0.58 USD more per plant for horticulture products grown in sustainable, nonpetroleum containers,[49] and (2) the projected growth of the bioplastics industry indicates increased production volume and reduction in price for PHA over the next decade.[50] Blends of PHA/PA with concentrations ≤50 wt % PA are good, affordable candidates for the horticulture-container application and should provide suitable strength, flexibility, and impact resistance, with a slower rate of biodegradation than pure PHA. Our results indicate that blends of PHA/PA possess mechanical properties that should also be applicable to many other industrial applications.

CONCLUSIONS

This study reports the results of evaluations with PHA/PA bio-based blends that were melt blended using a twin-screw extruder in order to improve the toughness of PHA and to characterize elemental properties of the blends. For all the samples studied by SEM, biphasic separation was observed, indicating that PHA was not miscible with PA in the melt. DMA results confirmed that the blend is a partially miscible two-phase system. Rheological results revealed that the melt viscosity of the blends increased with the content of PHA. On the basis of DSC results, both the melting and crystallization temperatures of the blends decreased systematically as the concentration of the PA increased. TGA

curves revealed that the thermal stability of the blends increased significantly at high temperatures as PA loadings increased. The elongation at break of PHA was greatly enhanced by the addition of PA due to the substantial decrease in the degree of crystallinity in the blends. Our results demonstrate that the flexibility and impact resistance of PHA can be improved significantly by blending with bio-based PA. The superior mechanical characteristics of PHA/PA blends make them strong candidates for use in crop containers that are biorenewable, yet can withstand the harsh conditions encountered during nursery-crop production. Blends of PHA and PA warrant consideration for other industrial applications where flexibility and impact resistance are essential, and biorenewable sourcing is preferred.

ACKNOWLEDGMENTS

This research was supported in part by the USDA Specialty Crops Research Initiative (NIFA-SCRI 2011-51181-30735), and by Iowa State University. The authors thank Metabolix, Inc. and Arizona Chemical Inc. for providing Mirel PHA and PA, respectively.

All of the authors meet the criteria for authorship in this journal. Shengzhe Yang contributed to the whole work, Samy A. Madbouly contributed the idea, and James A. Schrader contributed to the revision and funding. David Grewell, Michael R. Kessler, and William R. Graves contributed to the funding of this project.

REFERENCES

1. Albayrak, O.; Sen, S.; Cayli, G.; Ortac, B. *J. Appl. Polym. Sci.* **2013**, *130*, 2031.
2. Hoffendahl, C.; Fontaine, G.; Bourbigot, S. *Polym. Degrad. Stab.* **2013**, *98*, 1247.
3. Imre, B.; Pukanszky, B. *Eur. Polym. J.* **2013**, *49*, 1215.
4. Schiraldi, D. A.; Viggiano, R.; Chen, H. B. *Abstr. Pap. Am. Chem. Soc.* **2013**, 245.
5. Mulhaupt, R. *Macromol. Chem. Phys.* **2013**, *214*, 159.
6. Pion, F; Reano, A. F.; Ducrot, P. H.; Allais, F. *RSC Adv.* **2013**, *3*, 8988.
7. American Coatings Association, Inc. *JCT CoatingsTech* **2012**, *9*, 34.
8. Wang, D.; Sun, G. *J. Appl. Polym. Sci.* **2011**, *119*, 2302.
9. Haq, M.; Burgueno, R.; Mohanty, A. K.; Misra, M. *Compos. Part A Appl. Sci. Manufact.* **2011**, *42*, 41.
10. Shinohara, T.; Shirahase, T.; Murakami, D.; Hoshino, T.; Kikuchi, M.; Koike, J.; Horigome, M.; Masunaga, H.; Ogawa, H.; Takahara, A. *Buried Interface Sciences with X-Rays and Neutrons* **2011**, *2010*, 24.
11. Shi, D. J.; Chen, M. Q.; Akashi, M. *Appl. Chem. Eng.* Pts 1–3, **2011**, *236–238*, 2216.
12. Li, Y. F.; Liu, Y. X.; Fu, Y. L.; Wu, Q. L.; Wang, X. M. *Adv. Mater. Sci. Technol.* Pts 1 and 2, **2011**, *675–677*, 495.
13. Lee, K. Y.; Wong, L. L. C.; Blaker, J. J.; Hodgkinson, J. M.; Bismarck, A. *Green Chem.* **2011**, *13*, 3117.
14. Incoronato, A. L.; Buonocore, G. G.; Conte, A.; Lavorgna, M.; Del Nobile, M. A. *J. Food Prot.* **2010**, *73*, 2256.
15. Avella, M.; Buzarovska, A.; Errico, M. E; Gentile, G.; Grozdanov, A. *Materials* **2009**, *2*, 911.
16. Najer, A.; Wu, D. L.; Vasquez, D.; Palivan, C. G.; Meier, W. *Nanomedicine* **2013**, *8*, 425.
17. Ranquin, A.; De Vocht, C.; Van Gelder, P. *Polymer-Based Nanostructures: Medical Applications* **2010**, 315.
18. Malinova, V.; Meier, W. Polymer-Based Nanostructures: Medical Applications **2010**, 3.
19. Gerardand, T.; Budtova, T. *Eur. Polym. J.* **2012**, *48*, 1110.
20. Parulekar, Y.; Mohanty, A. K. *Macromol. Mater. Eng.* **2007**, *292*, 1218.
21. Shamala, T. R.; Divyashree, M. S.; Davis, R.; Kumari, K. S. L.; Vijayendra, S. V. N.; Raj, B. *Ind. J. Microbiol.* **2009**, *49*, 251.
22. Zheng, Z.; Deng, Y.; Lin, X. S.; Zhang, L. X.; Chen, G. Q. J. *Biomat. Sci. -Polym. Edn.* **2003**, *14*, 615.
23. Feng, F.; Ye, L. *J. Macromol. Sci. Part B Phys.* **2010**, *49*, 1117.
24. Deng, Y.; Zhao, K.; Zhang, X. F.; Hu, P.; Chen, G. Q. *Biomaterials* **2002**, *23*, 4049.
25. Kucharczyk, P.; Otgonzul, O.; Kitano, T.; Gregorova, A.; Kreuh, D.; Cvelbar, U.; Sedlarik, V.; Saha, P. *Polym. Plast. Technol. Eng.* **2012**, *51*, 1432.
26. Patel, M.; Gapes, D. J.; Newman, R. H.; Dare, P. H. *Appl. Microbiol. Biotechnol.* **2009**, *82*, 545.
27. Zhao, K.; Deng, Y.; Chen, J. C.; Chen, G. Q. *Biomaterials* **2003**, *24*, 1041.
28. Nam, S. Y.; Lee, Y. M. *J. Membr. Sci.* **1997**, *135*, 161.
29. Dave, V.; Tamagno, M.; Focher, B.; Marsano, E. *Macromolecules* **1995**, *28*, 3531.
30. Wang, Q.; Zhu, J. Y.; Wang, P.; Li, L. P.; Yang, Q.; Huang, Y. J. *J. Appl. Polym. Sci.* **2012**, *124*, 5064.
31. Dias, J. M. L.; Lemos, P. C.; Serafim, L. S.; Oliveira, C.; Eiroa, M.; Albuquerque, M. G. E.; Ramos, A. M.; Oliveira, R.; Reis, M. A. M. *Macromol. Biosci.* **2006**, *6*, 885.
32. Ahmad, E. E. M.; Luyt, A. S.; Djokovic, V. *Polym. Bull.* **2013**, *70*, 1265.
33. Bianchi, L.; Cimmino, S.; Forte, A.; Greco, R.; Martuscelli, E.; Riva, F.; Silvestre, C. *J. Mater. Sci.* **1985**, *20*, 895.
34. Greco, R.; Mancarella, C.; Martuscelli, E.; Ragosta, G.; Jinghua, Y. *Polymer* **1987**, *28*, 1929.
35. Tol, R. T.; Minakov, A. A.; Adamovsky, S. A.; Mathot, V. B. F.; Schick, C. *Polymer* **2006**, *47*, 2172.
36. Qiu, Z. B.; Komura, M.; Ikehara, T.; Nishi, T. *Polymer* **2003**, *44*, 7749.
37. Zhang, F.; McGinity, J. W. *Pharm. Dev. Technol.* **1999**, *4*, 241.
38. Zhao, Y.; Yang, D. C.; Vaughan, A. S. *Chem. J. Chin. Univ. Chinese* **1998**, *19*, 328.
39. Devireddy, R. V.; Leo, P. H.; Lowengrub, J. S.; Bischof, J. C. *Int. J. Heat Mass Trans.* **2002**, *45*, 1915.

40. Ladiwala, G. D.; Saxena, N. S.; Joshi, S. R.; Pratap, A.; Saksena, M. P. *Mater. Sci. Eng. A Struct. Mater. Prop. Microstruct. Process.* **1994**, *182*, 1427.

41. Nojima, S.; Akutsu, Y.; Akaba, M.; Tanimoto, S. *Polymer* **2005**, *46*, 4060.

42. Gumel, A. M.; Annuar, M. S. M.; Heidelberg, T. *Plos One* **2012**, 7.

43. Lazarewicz, T.; Haponiuk, J. T.; Balas, A. *E-Polymers* **2006**.

44. Kim, G. M.; Michler, G. H. *Polymer* **1998**, *39*, 5689.

45. Tseng, F. P.; Lin, J. J.; Tseng, C. R.; Chang, F. C. *Polymer* **2001**, *42*, 5063.

46. Bulakh, N.; Jog, J. P. *J. Macromol. Sci. Phys.* **1999**, *B38*, 277.

47. Gomez-Valdemoro, A.; San-Jose, N.; Garcia, F. C.; De La Pena, J. L.; Serna, F.; Garcia, J. M. *Polym. Chem.* **2010**, *1*, 1291.

48. Premraj, R.; Doble, M. *Ind. J. Biotechnol.* **2005**, *4*, 186.

49. Yue, C.; Hall, C. R.; Behe, B. K.; Campbell, B. L.; Dennis, J. H.; Lopez, R. G. *J. Agr. Appl. Econ.* **2010**, *42*(4), 757.

50. Voegele, E. *Biomass Magazine*, 16 October 2012. Available at: http://biomassmagazine.com/articles/8183/european-bioplastics-releases-2016-market-forecast.